Geotechnical Properties of Lower Rhine Silt

Propriétés géotechniques du limon du Rhin inférieur

by Edgar SCHULTZE, Professor Dr.-Ing.
and
Panaghiotis KOTZIAS, A.B., M.Sc., Athens, Technische Hochschule Aachen, Germany

Summary

During the last 12 years the Institut für Verkehrswasserbau, Grundbau und Bodenmechanik, Technische Hochshule Aachen has carried out an extensive testing programme of foundation investigations into the compressibility of the silt deposits in the lower Rhine Region.

These silts are late diluvial normally consolidated deposits. Stratigraphically and mineralogically they present a typical Loess formation. Their colour, texture, grain size and plasticity are strikingly similar to Loess formations in other parts of the world. However, their bulk density is greater and their degree of saturation is higher.

Many results of classification and compression tests have been compiled and compared with known results from silt deposits in other regions. The course of settlement and its relation to the most important soil index values has been statistically evaluated, revealing tendencies which would otherwise have remained undetected.

By means of empirical correlation between the compressibility constants and simple soil index values it is possible to estimate the settlement range of the silt. The equations developed can be used with sufficient accuracy for normal settlement calculations instead of single compression test results.

Sommaire

Au cours des 12 dernières années l'Institut de Verkehrswasserbau, Grundbau und Bodenmechanik, de la Technische Hochschule d'Aix-la-Chapelle a effectué, conjointement à ses analyses de terrains à bâtir, des recherches approfondies sur les propriétés de tassement des dépôts de limon de la région du Rhin inférieur.

Le limon de la région du Rhin inférieur est un dépôt normalement consolidé, datant de la fin du diluvien. Du point de vue stratigraphique et minéralogique il présente l'aspect typique d'une formation de loess. Sa couleur, sa texture, sa granulométrie et sa plasticité lui confèrent une ressemblance frappante avec d'autres formations de loess qui se rencontrent dans différentes régions du globe. Cependant il se distingue de ces formations par sa plus grande compacité et son degré de saturation plus élevé.

Les nombreux résultats donnés par les essais de classification et de compressibilité ont été groupés et comparés à d'autres résultats de recherches connus, provenant d'autres gisements.

La compressibilité de ce limon et ses relations avec les principales caractéristiques géotechniques ont été évaluées à l'aide de méthodes statistiques. C'est ainsi qu'il a été possible de découvrir des tendances inconnues avant ces recherches

A l'aide de relations trouvées empiriquement entre les valeurs caractéristique de la compressibilité et les constantes simples du sol, il est possible d'estimer aisément l'ordre de grandeur de tassement des limons. Les équations de déterminations peuvent être appliquées avec une exactitude suffisante pour des calculs de tassement normaux et celà sans faire des essais de compression.

1. Introduction

The Rhine silt belongs to an extensive stratum of loess which cuts across Europe. This originated mainly during the glacial stages when arid climates and steppes predominated. It is a deposit resulting from large dust clouds formed of weathered rock material and has, thus a fairly uniform grain size (Fig. 1). The Rhine silt, however, is a secondary loess in the sense that after repeated weathering, blowing and washing away, it was finally deposited. In contrast to primary loess, a direct wind deposit, it has relatively high bulk density and a low lime content, and is normally consolidated. It originated in the Quaternary period during the Würm glaciation. Its greatest stratum thickness is 30 m. From a soil mechanics point of view it is a sandy silt with a small proportion of clay, which is active. It belongs to the *CL-ML* group of the uniform classification system.

Since this soil has often been investigated for construction projects during the past twelve years, 270 to 360 samples have been statistically examined. The purpose of this was to provide a closer appreciation of the variation in its index properties and to gain an insight into the laws governing its compressibility.

2. Frequency distribution of soil index properties

By means of frequency diagramms the individual soil index properties have been presented (Figs. 2-4). The fluctuations

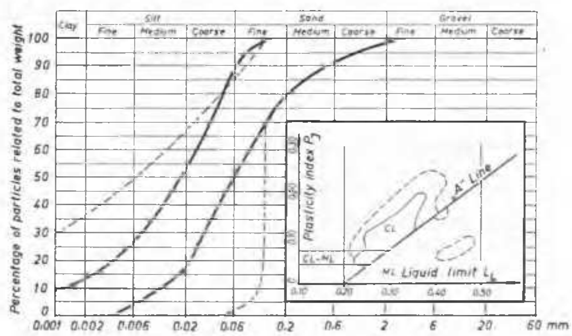

Fig. 1 Range of grain-size distribution and plasticity chart of Rhine silt.
——— 70 per cent of all tests
-·-·-·- 100 per cent of all tests
Granulométrie et carte de la plasticité du limon rhénan.
——— 70 pour cent de tous les essais
----- 100 pour cent de tous les essais

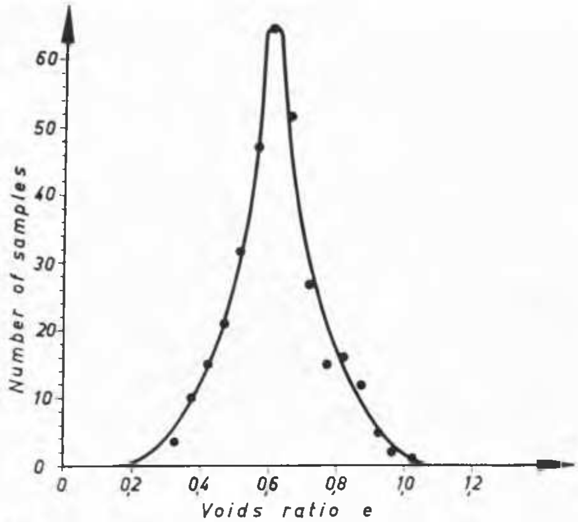

Fig. 2 Frequency diagram for initial void ratio in an undisturbed state.

Number of samples	$N = 334$
Mean value	$\bar{X} = 0{\cdot}651$
Standard deviation	$\bar{\sigma} = 0{\cdot}186$
Variance	$\bar{R} = 0{\cdot}30 — 1{\cdot}75$

Diagramme de la fréquence pour les indices des vides dans l'état non remanié.

Nombre des échantillons	$N = 334$
Valeur moyenne	$\bar{X} = 0{,}651$
Ecart moyen	$\bar{\sigma} = 0{,}186$
Variation	$\bar{R} = 0{,}30 — 1{,}75$

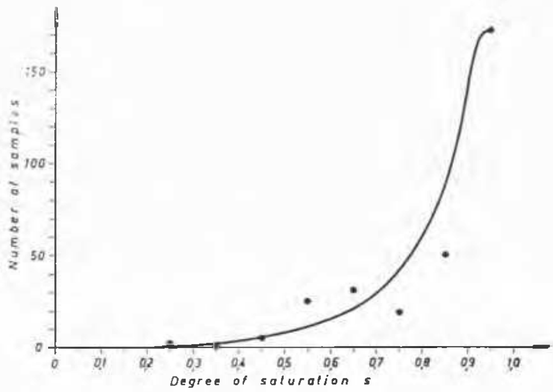

Fig. 3 Frequency diagram for the degree of saturation of undisturbed soil.

Number of samples	$N = 334$
Mean value	$\bar{X} = 0{\cdot}845$
Standard deviation	$\bar{\sigma} = 0{\cdot}163$
Variance	$\bar{R} = 1{\cdot}0 — 0{\cdot}225$

Diagramme de la fréquence pour le degré de saturation du sol remassié.

Nombre des échantillons	$N = 334$
Valeur moyenne	$\bar{X} = 0{,}845$
Écart moyen	$\bar{\sigma} = 0{,}163$
Variation	$\bar{R} = 1{,}0 — 0{,}225$

of the various soil properties are given by their average and the standard deviation (Table 1).

3. Time/settlement curve

An analysis of the time-compression curve indicates that from the total consolidation, 47 per cent is initial, 28 per cent

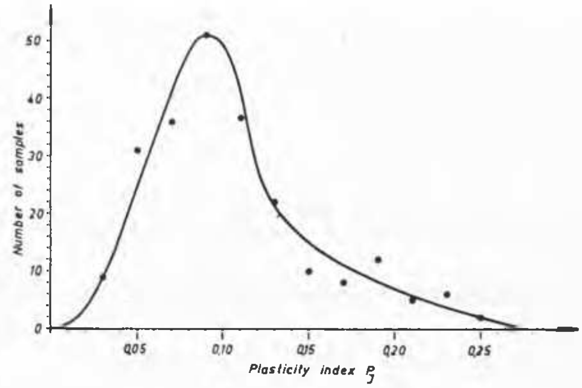

Fig. 4 Frequency diagram for plasticity index.

Number of samples	$N = 236$
Mean value	$\bar{X} = 0{\cdot}114$
Standard deviation	$\bar{\sigma} = 0{\cdot}061$
Variance	$\bar{R} = 0{\cdot}02 — 0{\cdot}26$

Diagramme de la fréquence pour la plasticité.

Nombre des échantillons	$N = 236$
Valeur moyenne	$\bar{X} = 0{,}114$
Écart moyen	$\bar{\sigma} = 0{,}061$
Variation	$\bar{R} = 0{,}02 — 0{,}26$

Table 1

Average values for index properties of Rhine silt
Caractéristiques géotechniques moyennes du limon rhénan

Index property	*Dimens.*	*Symbol.*	*Number of samples*	*Average*	*Standard Deviation*
Average grain size	mm	D 50	258	0·03	0,02
Effective grain size	mm	D 10	229	0·005	0,003
Uniformity coefficient	1	U	272	13	12
Specific gravity	g/cm³	G_s	316	2,66	0·04
Natural bulk density	g/cm³	γ	409	1·97	0·12
Natural void ratio	1	e_n	334	0·65	0·19
Natural water content	%	w_n	419	21	5
Degree of saturation	%	s	334	85	16
Liquid limit	%	L_L	236	29	7
Plasticity index	%	P_I	236	11	6
Flow Index	%	I_F	192	9	3
Toughness Index	1	T_w	185	1·35	0·62
Consistency Index	%	C_I	262	73	32
Activity	1	A	171	1·9	1·5
Modulus of compressibility (p = 0·65-2·60	kg/cm²	$Es = \frac{1}{m_v}$	186	96	35
Coeff. of consolidation	cm²/s	c_v	80	0·004	0·002
Endtime of primary consolidation (Height of sample 1·4 cm)	min	t_p	317	3	2

is primary and 24 per cent is of a secondary nature. In a sample of 1·4 cm height the primary consolidation is completed after $3{\cdot}3 \pm 2{\cdot}1$ minutes.

The load is therefore maintained for only a short time. On the average, the load was increased every hour in the compression test.

From the time-compression curve it was further estimated that the permeability of this soil is of the order of magnitude $k = 10^{-8}$ cm/sec instead of 10^{-5} to 10^{-7} cm/sec as obtained from permeability tests.

The coefficient of permeability, estimated indirectly from the time/settlement curve, is evidently too low.

4. Stress-strain curve

In contrast to many American silts which display relatively high settlements when water is added, the Rhine silts are stable upon saturation (Fig. 5). This is due to the fact that their initial void ratio is generally less than 0·85. In agreement with the geological history of this formation, the compression tests reveal a preconsolidation pressure consisting only of the weight of overlying soils which is generally very small (Fig. 8).

The most significant part of the stress-strain curve for investigation, is therefore the virgin compression curve.

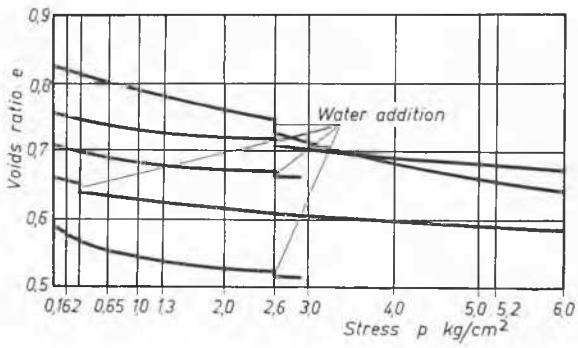

Fig. 5 Influence of water addition on the stress-strain curve of Rhine silt for various initial void ratios. Water addition at a degree of saturation of 0·45 — 0·98.

Influence de l'adjonction d'eau sur la courbe de compression des limons rhénans avec l'indice des vides initial et different. Adjonction d'eau à un degré de saturation de 0,45 — 0,98.

5. Equation of the stress-strain curve

5.1. *Initial compression.*

From the results of the investigation the initial part of the stress-strain curve (Fig. 6) can be given with sufficient accuracy by the equation :

$$E_s = \frac{1}{m_v} = vp^w$$

$E_s = \dfrac{1}{m_v}$ = Modulus of compressibility (confined compression test) p = stress (kg/cm²).

From this equation for the modulus of compressibility the following equations for the settlement are derived.

$$\text{for } w \neq 1 : \varepsilon = \frac{1}{v(1-w)} p^{1-w} + C = ap^k + C \qquad \ldots\ldots (2)$$

$p = 0 : \varepsilon = 0 : C = 0$
$p = 1 : \varepsilon = a$
$p = 1 : \varepsilon = a$

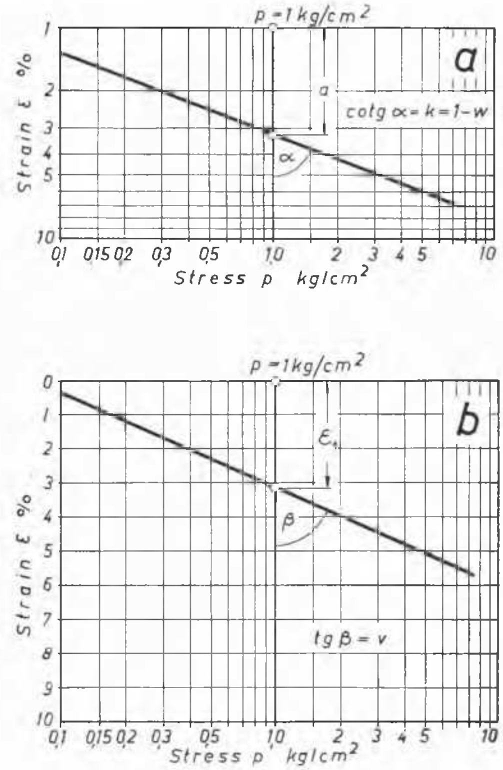

Fig. 6 Typical stress-strain curve for silt.
a) double logarithmic scale
b) single logarithmic scale.

Courbes typiques de compression du limon.
a) représentation doublement logarithmique
b) représentation semi-logarithmique.

$$\log_e \varepsilon = \log_e a + k \cdot \log_e p \qquad (2a)$$

$$\text{for } w = 1 : \varepsilon = \frac{1}{v} \log_e p + C \qquad \ldots\ldots (3)$$

$$p = 1 : \varepsilon = C = \varepsilon_1$$

$$\varepsilon = \frac{1}{v} \log_e p + \varepsilon_1 \qquad \ldots\ldots (3a)$$

The relationships between the various constants (Figs. 6a, 6b) are as follows :

$$v = \frac{1}{ak} \qquad w = 1 - k \qquad (4)$$

$$a = \frac{1}{v(1-w)} \qquad k = 1 - w \qquad (5)$$

The constants v, w, and a, k respectively were estimated by means of correlation analysis.

For the estimation of the exponent w, it was found suitable to use a coordinate system in which the abscissa gives the relative compression ε_p under a load p and the ordinate gives the corresponding compression under a double loap ε_{2p}. In this coordinate system the test results are plotted as points. In a linear scale a very good relationship is attained for the various loading increments (Fig. 7).

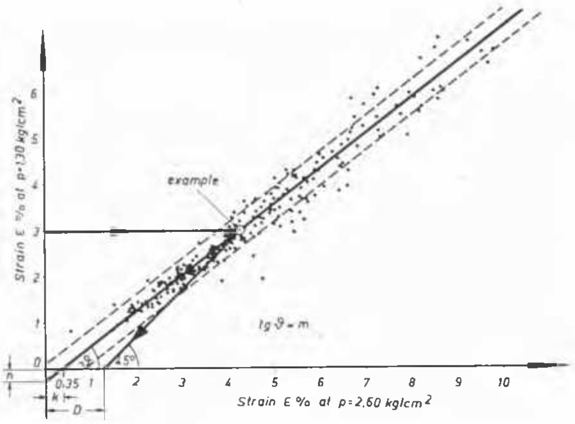

Fig. 7. The interrelation between the strain under the stress 1·3 and 2·6 kg/cm².
Rapport entre la compression à la pression de 1,3 et 2,6 kg/cm².

The resulting straight lines can be given by the equations :

$$\varepsilon_p = \frac{1}{2^k}\,\varepsilon_{2p} - C\,\frac{1-2^k}{2^k} \tag{6}$$

$$\varepsilon_p = m\varepsilon_{2p} - n \text{ or } \varepsilon_{2p} = m'\varepsilon_p + n' \tag{6a}$$

$$m = \frac{1}{2^k} = \frac{1}{2^{1-w}} \tag{7}$$

$$\log_e m = \log_e 1 - (1-w)\log_e 2 \tag{7a}$$

$$k = 1 - w = \frac{\log_e 1 - \log_e m}{\log_e 2} = \frac{\log_e(1/m)}{\log_e 2} \tag{8}$$

$$w = 1 - \frac{\log_e(1/m)}{\log_e 2} \tag{9}$$

Similarly w' is obtained from m'

The values of w differ only slightly for the investigated lines for loading increment and thus fluctuate irregularly indicating no relationship with the stress.

The same holds true also for w' (Table 2). There is a strong relationship between the compressions in accordance with equation (6). This can be inferred from the high coefficients of correlation which are all more than 0·95 thus indicating an almost functional relationship.

Table 2

Results of correlation analysis between ε_p et ε_{2p} - p = stress, N = Number of samples, R = coefficient of correlation

Résultats de la comparaison entre ε_p et ε_{2p} - p = pression, N = nombre des échantillons, R = coefficient de comparaison.

p	$2p$	R	N	m	w	m'	w'	w_m	w
kg/cm²	kg/cm²	1	1	1	1	1	1	1	1
0·162	0·325	0·963	267	0·736	0·56	1·261	0·65	0·60	↑
0·325	0·65	0·971	264	0·749	0·58	1·258	0·67	0·62	0·62
0·65	1·3	0·974	272	0·748	0·58	1·267	0·64	0·61	
1·3	2·6	0·951	259	0·769	0·62	1·185	0·71	0·65	↓
2·6	5·2	0·956	239	0·744	0·57	1·129	0·70	0·63	
5·2	10·4	0·973	154	0·784	0·65	1·208	0·74	0·69	

It can be concluded that in equation (I) the exponent w—in contrast to the sand discussed in the paper of Schultzer—Moussa, is almost constant. It lies midways between w and w' and is 0·62 for the usual range of loading. It is possible, in a double logarithmic scale to give the stress-modulus of compressibility equation of this silt as a straight line which has the same slope for all soil samples. The individual silt samples differ only in the coefficient v.

5.2. *Rebound and recompression.*

All rebound curves, and with a good approximation the recompression curves, are straight lines. This means that the exponent $w = 1$, which corresponds to the presentation given in Fig. 7 at an angle of 45°. Equation (3), therefore, gives the curve of compression and rebound.

5.3. *Estimation of the preconsolidation pressure.*

The usual method of estimating the preconsolidation pressure in clays through the stress-strain curve, such as that of Casagrande method is not applicable to the equation $E_s = \frac{1}{m_v} = vp^{0.62}$. The stress-strain curve is in this case already curved without any preconsolidation pressure. It is possible, however, to estimate the preconsolidation pressure by plotting, for the same soil sample, the diagramm $\varepsilon_p/\varepsilon_{2p}$ of Fig. 8. The intersection of both straight lines gives the preconsolidation pressure, which corresponds to the overburden pressure on the soil.

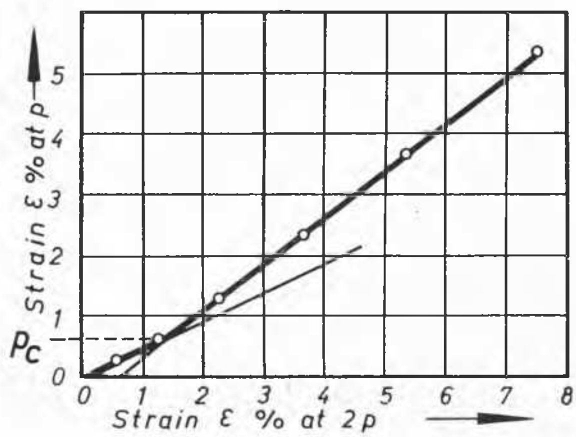

Fig. 8 Determination of the pre-consolidation pressure of a silt.
Détermination de la pré-consolidation d'un limon.

6. Estimation of the coefficient v

From equation (2) and for any point the magnitude of the coefficient v can be derived as follows (Fig. 7).

$$\varepsilon_p = ap^k$$
$$\varepsilon_{2p} = a2^k p^k$$
$$\varepsilon_{2p} = \varepsilon_p + ap^k(2^k - 1) = \varepsilon_p + D \tag{10}$$

It follows therefore : that

$$a = \frac{D}{p^k \cdot (2^k - 1)} \tag{11}$$

$$v = \frac{1}{ak} = \frac{p^k \cdot (2^k - 1)}{kD} \qquad (12)$$

The value of D is estimated graphically from Fig. 7. Each point of the presentation of Fig. 6 has a different v.

The coefficient v shows considerable scattering and depends upon the soil properties. By means of correlation analysis, the following relationships have so far been investigated.

Between $\log_{10} v$ and natural water content w_n we have :

$$\log_{10} v = 2{\cdot}13 - 0{,}018 w_n$$

The coefficient of correlation is 0,488. Another relationship was obtained graphically and is :

$$\log_{10} v = 3 - 0{,}85 \log_{10} w_n$$

Between $\log_{10} v$ and the liquid limit L_L there is a correlation coefficient of 0·277. Similarly, between $\log_{10} v$ and the plastic limit P_L the coefficient of correlation if 0·289 and between v and the consistency index C_I the coefficient is 0·380. All these coefficients of correlation are too low to enable v to be estimated through a single index property of the soil.

The relationship between v and the soil index properties is estimated most accurately through a multiple correlation between v or $\log_{10} v$ and the following. Initial void ratio e, degree of saturation s, and plasticity index P_I. The investigations of this relationship have not so far been completed.

Conclusion

The typical stress-strain curve of the clay is not observable in silts. In clays w is usually taken as 1 and the preconsolidation pressure is estimated through a tangent construction. In the case of silt this leads to inaccurate results. The rebound curve reveals conditions similar to these found in other soils. The exponent of the equation $E_s = \frac{1}{m_v} = v p^w$ is almost constant in silt and is independant of the properties of each sample. On the other hand, the coefficient v is quite dependent from the porosity, the natural water content, and the grain size particularly for the amount of clay (plasticity index) present as well as the activity of the individual clay particles. The estimation of this coefficient from other soil properties has not so far been attempted.

8. Acknowledgment

Mr. Hollmann cand. ing. and Mr. Schmerbitz cand. ing. have contributed to the statistical evaluation of the test results and in the performance of the complementary tests. Their collaboration is fully appreciated.

9. References

[1] Kotzias (1959). Der rheinische Schluff als Baugrund. Mitteilungen aus dem Institut für *Verkehrswasserbau, Grundbau und Bodenmechanik der Technischen Hochschule Aachen*, Heft 20 : Baugrundkursus 1959, pp. 82.

[2] —(1960). Die Zusammendrückbarkeit des rheinischen Schluffs *Dr Thesis. Technische Hochshule Aachen.*